



OPEN

Predicting 3D and 2D surface area of corals from simple field measurements

Josie F. Chandler^{1✉}, Will F. Figueira², Deborah Burn¹, Peter C. Doll¹, Abby Johandes¹, Agustina Piccaluga² & Morgan S. Pratchett¹

The structural architecture of coral reefs is a known predictor of species richness, fish biomass and reef resilience. At a smaller scale, three-dimensional (3D) surface area of corals is a fundamental determinant of physical and biological processes. Quantifying the 3D surface area of corals has applications for a broad range of scientific disciplines, including carbonate production estimates, coral predation studies, and assessments of reef growth. Here, we present morphotaxon-specific conversion metrics to estimate total 3D surface area and projected 2D surface area of individual colonies from simple field measurements of colony maximum diameter. Underwater photogrammetry techniques were used to quantify surface area and estimate conversion metrics. Bayesian models showed strong non-linear (power) relationships between colony maximum diameter and both total 3D surface area and projected 2D surface area for 13 out of 15 morphotaxa. This study presents a highly resolved and efficient method for obtaining critical surface area assessments of corals for various applications, including assessments of biotic surface area, tissue biomass, calcification rates, coral demographic rates, and reef restoration monitoring.

Scleractinian corals form the framework of tropical coral reefs, providing structure for essential habitats, including for critical early life stages of both ecologically and economically important species^{1–3}. Additionally, coral reefs provide valuable ecosystem goods and services to tropical and subtropical nations; their structures forming natural barriers to oceanic wave energy, buffering shorelines from erosion and flooding^{4,5} as well as providing protein and income for coastal communities^{6,7}. As the most widely used indicator of reef health, coral cover has been estimated using a variety of methodologies which are largely based on measuring the relative abundance (and size) of benthic substrate types⁸. The two-dimensional (2D) surface area of coral, or the area of occupancy, is commonly estimated based on simple field measurements (e.g., point-intercept or line-intercept methods⁹). Notably, the ubiquity of 2D (planar) representations of benthic communities facilitates standardization and comparison between and within different reef monitoring programs¹⁰.

While 2D approaches continue to be useful for fast estimates and comparisons of benthic cover and composition^{15,16}, they are lacking in a third dimension which provides insight into the structural complexity of corals and reefs. Given that the morphological complexity of corals is a key determinant of habitat facilitation for reef organisms^{1–3}, the inclusion of three-dimensional (3D) structure in reef health assessments incorporates an aspect of ecosystem health which is overlooked by using planar estimates of coral cover alone. Quantifying the structural complexity of coral reefs is increasingly recognized as an important aspect of ecosystem monitoring, as topographic complexity is not only a key driver of biodiversity and productivity of reef ecosystems^{11–14}, but also has consequences for calcification rates, wave attenuation potential and other reef functions. The dual process of coral growth and skeletal erosion drive changes in habitat structure over time which is important for understanding evolving reef function^{15,16}. As such, surveys that fail to incorporate 3D aspects of coral reefs into data collection are overlooking important ecological parameters.

The 3D complexity of individual coral colonies is a necessary component to describe the surface area of live tissue and understand biological processes such as metabolism, photosynthesis, reproductive potential, and nutrient uptake^{20–22}. Moreover, precise quantification of live tissue and other 3D characteristics of individual colonies facilitates assessment and modelling of key demographic processes, including the growth and reproduction of coral colonies^{17,18}. Surface area is, therefore, a valuable metric for both the monitoring and modelling of these colony-level processes.

¹College of Science and Engineering, James Cook University, Townsville, QLD 4811, Australia. ²School of Life and Environmental Sciences, University of Sydney, Sydney, NSW 2006, Australia. ✉email: josie.chandler@my.jcu.edu.au

Researchers have been attempting to estimate surface area of individual coral colonies since as early as the 1950s¹⁹. Accurately capturing the fine-scale complexity of the coral structures, however, has proven difficult. Early methods used geometric approximations based on shapes comparable to coral morphologies¹⁹. This work was followed by surface indices (SI) or ‘scaling factors’ which converted field measurements of colony diameter and planar area to 3D surface area, using theoretical approximations^{20,21}. The conversions were based on crude geometric representations of shapes such as hemispheres, discs, and branched cylinders to approximate ‘massive’, ‘plate-like’, and ‘branched’ coral morphologies, respectively. The resulting surface area estimates invariably underestimate true surface area^{22,23}, especially for complex growth forms. Despite these limitations, the SI concept demonstrated the potential for applying pre-determined mathematical relationships to measured parameters for surface area estimates. Additional techniques attempting to quantify 3D surface area of corals have included wrapping colonies in aluminium foil and subsequently measuring the area of material required to cover the surface of the coral²⁴, dipping corals in either paraffin wax²⁵, dye²⁶ or latex²⁷, then removing the liquid coating and measuring the volume of the liquid, and more recently the use of CT scans and X-rays²³. Whilst some of these methods (i.e., wax dipping) were found to produce relatively accurate and repeatable estimations of surface area²⁸, most methods were underestimating the complex corallite architecture of the corals and consequently underestimating the actual coral tissue surface area. Another drawback of these methods was that they required the collection and destruction of the colony.

In recent years, the revolution of modern aquatic photogrammetry techniques^{29,30} has enabled in situ assessments of coral surface area to be calculated through a non-destructive and highly resolved method. In comparison to traditional methods of measuring coral surface area, photogrammetry has been proven to produce data with higher precision and lower error^{31,32}, alongside enabling extraction of additional metrics such as volume and shelter capacity³³. The drawback, however, is that the process of photogrammetry is time consuming and requires specialist software and training^{16,34}, as well as some reliance on favourable environmental conditions (e.g., currents, swell, visibility). Recent advances in photogrammetry have enabled mapping of relatively large spatial scales (hundreds of square metres³⁵) with high accuracy and precision, which can provide information on habitat structural complexity and demographic rates, including at an individual colony level^{30,31,35}. However, the time and processing power required to render and analyse these data-heavy models can be restrictive, especially if timely data generation is required^{31,35,36}. Conversely, lower resolution measurements, such as the diameter of coral colonies, are fast and easy to obtain, and they can be collected either via in situ tape measurements or alternatively obtained from photographs, even from historical datasets.

The objective of this paper was to take advantage of opportunities afforded by photogrammetry to quantify total 3D surface area and projected 2D surface area of different coral morphotaxa, and to test how these parameters relate, to explore opportunities to rapidly estimate total 3D surface area and projected 2D surface area of different coral morphotaxa, based on simple field-based measurements (colony maximum diameter). Whilst this is not the first study to describe the relationship between coral diameter and 3D surface area of corals^{10,21,34,37,38}, previous studies have only converted a small number of broad-level coral morphologies. For example, House et al.¹⁰ established predictive relationships between 2D and 3D surface area, specific to three broad morphotypes (‘branching’, ‘encrusting’ and ‘massive’) based on a total of 22 specimens, however these broad groupings do not adequately capture the morphological heterogeneity of coral species in the Indo-Pacific. More recently, Aston et al.³⁷ established predictive relationships between planar area and a whole suite of 3D structural metrics in addition to surface area (volume, spatial refuge, shelter size factor, etc.), for seven morphotaxa of corals on the GBR (‘Branching *Pocillopora*’, ‘Digitate *Acropora*’, ‘Corymbose *Acropora*’, ‘Tabular *Acropora*’, ‘Massive’, ‘Branching *Isopora*’ and ‘Branching *Porites*’), built from the photogrammetry of 69 specimens. The morphotaxa presented in the study were more refined than the morphotype groupings used by House et al.¹⁰, but do not encompass the full range of morphologies present in the region, meaning some coral forms (e.g., staghorn *Acropora*, encrusting corals) cannot be modelled using these published relationships.

Here, taxon-specific conversion metrics are provided, with morphotaxa categories encompassing all common scleractinian corals on Australia’s Great Barrier Reef (GBR). We present equation parameters for 12 specific morphotaxa and three ‘Other’ categories, enabling surface area metrics to be extracted by any researcher with measurements of colony diameter from field surveys or photographs. This information can be used by researchers and managers to provide a more rigorous representation of available coral as community habitat and tissue biomass, and for estimating biological and physical processes of corals. It also presents an opportunity to assess fine-scale changes in colony growth and recovery²¹ at a reef level.

Methods

Data collection

To construct relationships between simple linear measurements of colony maximum diameter and colony surface area (both projected 2D surface area and total 3D surface area), predictive models for various morphotaxa were built. Measurements of colony maximum diameter were collected in the field and surface area metrics were extracted in the lab using 3D photogrammetry software.

Field sampling for this study was conducted at Lizard Island (14°40’S, 145°27’E) in the northern Great Barrier Reef, Australia, in November and December 2023. Corals were selected from five sites (between 2–10m depth); namely North Point, Granite Bluff, Turtle Beach, Casuarina Beach and Big Vicki’s on the North-West and West of the Island.

10 coral genera (*Acropora*, *Astreopora*, *Fungia*, *Goniastrea*, *Lobophyllia*, *Montipora*, *Pocillopora*, *Porites*, *Seriatopora* and *Stylophora*) were pre-selected due to their dominance on coral reefs around Lizard Island, collectively accounting for 84.45% of hard coral cover based on Point Intercept Transect (PIT) surveys at these sites, as per methodology outlined by Hill & Wilkinson⁹. Due to the morphological heterogeneity of *Acropora* spp. this genus

was further split into the three common morphotaxa ‘*Acropora*—table’, ‘*Acropora*—staghorn’ and ‘*Acropora*—Other’, and for the genera *Montipora* and *Porites* the dominant growth forms were specified as ‘*Montipora*—encrusting’ and ‘*Porites*—massive’. To establish relationships for corals which were not encompassed by these 12 morphotaxa groups, corals from less common genera were haphazardly chosen and later grouped together to form three ‘Other’ morphotaxa: ‘Other—branching’, ‘Other—encrusting’ and ‘Other—massive’. Here, ‘massive’ was defined as colonies with a hemispherical structure, ‘encrusting’ was defined as colonies with low relief that grow against the substrate and ‘branching’ was defined as colonies that have numerous branches, usually including secondary branches which are smaller offshoots growing from the primary branches.

The resulting 15 morphotaxa modelled in this study were: *Acropora*—other (n = 13 colonies), *Acropora*—staghorn (n = 14), *Acropora*—table (n = 13), *Astreopora* (n = 9), *Fungia* (n = 6), *Goniastrea* (n = 11), *Lobophyllia* (n = 10), *Montipora* encrusting (n = 11), *Pocillopora* (n = 13), *Porites*—massive (n = 9), *Seriopora* (n = 9), *Stylophora* (n = 10), *Other—branching* (n = 6), *Other—encrusting* (n = 13), and *Other—massive* (n = 12). Replicates for each morphotaxon were determined based on the structural complexity and morphological variation within each morphotaxon. For morphotaxa with open and complex growth forms (i.e., *Acropora*—staghorn), a disproportionately higher number of replicates were used, to account for predicted uncertainty in model fit. In contrast, for morphotaxa with relatively consistent morphology (i.e., *Fungia*), fewer replicates were required because surface area was expected to scale quite consistently with size. Where possible, replicate colonies were selected over an even spread of size classes from small to large. In total, models were built for 159 colonies across the 15 morphotaxa.

For each of the 15 morphotaxa, we established relationships between a) colony maximum diameter and projected 2D surface area and b) colony maximum diameter and total 3D surface area. For each coral colony, in situ measurements of colony maximum diameter were taken using a tape measure based on the longest length, with only living tissue included in the measurements. Where necessary, multiple measurements were taken to determine colony maximum diameter. For all morphologies, colonies were measured from a planar perspective rather than wrapping around the colony contour. Field measurements of colony maximum diameter ranged from 3 to 150 cm. After measurements were taken, each colony was imaged for 3D modelling (see ‘[Model reconstruction and data extraction](#)’).

Model reconstruction and data extraction

GoPro Hero 11 Black cameras were used to collect close-range imagery of individual colonies for 3D modelling. Structure from motion techniques (SfM) were followed, as described by Ferrari et al.¹⁵. However, instead of time-lapse imagery, we used 4K video footage (30fps) for faster in-water data collection, enabling more replicates per morphotaxon. Additionally, custom-built scaling objects (Agisoft Metashape coded targets, 12bit, inverted, 20% of full size, target centres 60 mm apart) were incorporated into the scene. Image acquisition involved filming the colony from all angles, moving in a sweeping motion to form arcs from top to bottom. Agisoft Metashape v 1.7.6 software was used for processing of videos and model building. Jpeg frames were extracted from the 4k videos every 4th frame. Videos varied in length according to the size and complexity of corals being filmed, where larger and/or more complex corals required more thorough and lengthy videos to capture full extent of colony surface area. Accordingly, image sets used to build 3D models varied in size. Mean video length was 1 min, while image sets ranged from 150 to 1400 images.

Three dimensional models were reconstructed from image sets using Agisoft Metashape software (parameters outlined in Appendix 1, Supplementary Material, Table S1). Models were scaled using at least two sets of independent scale bars (60 mm in length) from the coded target objects described above. Resulting models had an average mesh resolution (distance between vertices) of 1.86 mm and average ground sample distance of 0.178 mm/pixel. Any extraneous mesh material that was not part of the colony was removed using Agisoft Metashape selection tools. Colony 3D surface area was extracted using the Mesh-Area tool in Agisoft Metashape. In order to extract 2D surface area, the model was first projected onto a 2D plane, in the same aspect as a top-down image taken of the colony in situ. To do this, we visually oriented the models in the software to replicate a top-down field of view, where the z-axis was aligned perpendicular to this view plane (e.g., Fig. 1a–c). Once this was done, the 2D area of the colony was estimated using the Export Report tool within the software with projection set to the X–Y plane.

Statistical models

The relationships between colony maximum diameter and surface area metrics were explored for each morphotaxon using Bayesian generalized linear modelling (GLM) with a gaussian distribution. An approximate power-law relationship between coral maximum diameter and surface area was assumed based on underlying geometric properties of corals as well as evidence in the literature for allometric power-scaling relationships of corals^{16,37,39}. Logarithmic transformations were performed for both variables to meet model assumptions and the power-law of these relationships allowed for a linear regression model to subsequently be fitted. Specifically, log-transformed linear length data (field measurement of colony maximum diameter, cm) was modelled against log-transformed projected 2D surface area (cm²) or against log-transformed total 3D surface area (cm²). Weakly informative priors were selected based on visual exploration of the data following transformation. Bayesian posteriors were generated via a No-U-Turn Sampler (NUTS), run with three Markov Chain Monte Carlo (MCMC) chains, each for 15,000 iterations (excluding the first 5000 warm-up samples) with a thinning rate of 12. All chains were found to be well-mixed and converged (all Rhat < 1.01) on a stable posterior and were validated using the ‘DHARMA’ package⁴⁰ residuals and posterior probability checks. Data were back-transformed to the original scale after modelling for ease of parameter interpretation. To visualise the regression models, the posterior distribution for each morphotaxon was summarized with median lines using the ‘posterior_predict’ function.

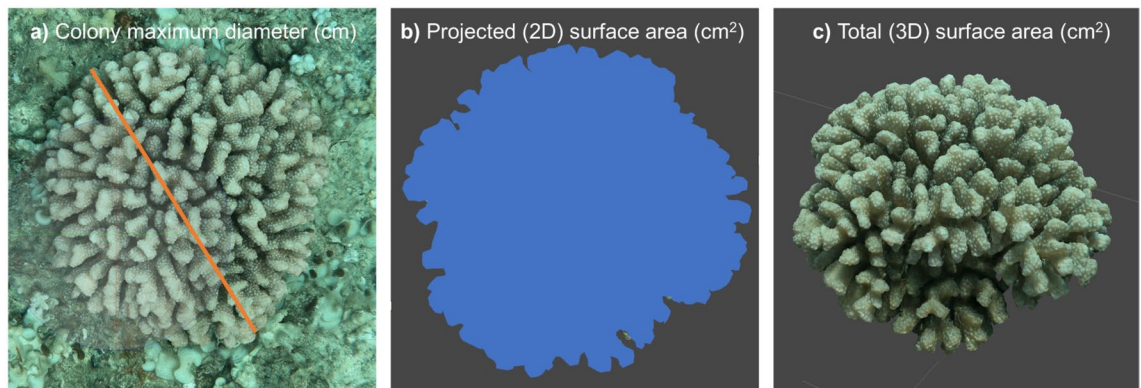


Fig. 1. (a) Field measurements of colony maximum diameter (cm), (b) projected 2D surface area (cm²) and (c) total 3D surface area (cm²) of the same coral colony. Images taken from Agisoft Metashape v 1.7.6 software during model reconstruction.

To demonstrate the range over which the posterior distribution credibly lies, for interpretation of model uncertainty, we incorporated bands of probability into the key figures (Figs. 3 & 4) representing different Highest Density Intervals (HDIs 0.99, 0.95, 0.8, 0.5). HDIs represent the range within which a specified proportion of the posterior distribution falls; i.e. 0.95 HDI band encompasses 95% of the posterior distribution. Narrower HDIs denote more precise model estimates. Highest Density Intervals were calculated and visualized using the ‘tidybayes’ package.

Tables were produced to present model predictions over a range of field measurements for each morphotaxon, as an easily interpretable presentation of modelled data. Each predicted value (estimated marginal means, ‘emmeans’) was presented together with the range of credible values (as 95% HPDs) for that estimate. These tables are presented in Supplementary material (Appendix 2, Tables S2-16) and were designed to be used by practitioners for interpreting the range of uncertainty around their model estimates for given sizes/morphotaxon. Emmeans were calculated using the ‘emmeans’ package⁴¹. All statistical models were performed in R version 4.3.1⁴² via the ‘brms’ package⁴³.

Results

To assess the utility of rapid field measurements of colony maximum diameter, it was first necessary to establish the capacity to consistently and accurately measure colony diameter in the field. To validate this approach, field measurements of colony length were compared to estimates of colony maximum diameter extracted from 3D models, with results indicating a very high correlation (Fig. 2, $R^2 = 0.97$).

Strong non-linear (power) positive relationships (Bayesian R^2 values > 0.9 ; Table 1) between rapid field measurements of colony maximum diameter and projected 2D surface area were observed for 13 of the 15 morphotaxa. These include *Acropora*—other ($R^2 = 0.99$), *Acropora*—table ($R^2 = 0.95$), *Astreopora* ($R^2 = 0.94$), *Fungia* ($R^2 = 0.99$), *Lobophyllia* ($R^2 = 0.97$), *Montipora*—encrusting ($R^2 = 0.95$), *Pocillopora* ($R^2 = 0.94$), *Porites*—massive ($R^2 = 0.91$), *Seriatopora* ($R^2 = 0.97$), *Stylophora* ($R^2 = 0.96$), Other—branching ($R^2 = 0.94$), Other—encrusting ($R^2 = 0.96$) and Other—massive ($R^2 = 0.96$) (Fig. 3). While to a lesser extent, a positive relationship was also identified for *Acropora*—staghorn ($R^2 = 0.84$) and *Goniastrea* ($R^2 = 0.89$) (Fig. 3, Table 1).

Strong non-linear (power) positive relationships (Bayesian R^2 values > 0.9 ; Table 1) between colony maximum diameter and total 3D surface area were observed for 11 of the 15 morphotaxa. These include *Acropora*—other ($R^2 = 0.95$), *Acropora*—table ($R^2 = 0.95$), *Fungia* ($R^2 = 0.96$), *Lobophyllia* ($R^2 = 0.96$), *Montipora*—encrusting ($R^2 = 0.92$), *Pocillopora* ($R^2 = 0.95$), *Seriatopora* ($R^2 = 0.97$), *Stylophora* ($R^2 = 0.96$), Other—branching ($R^2 = 0.96$), Other—encrusting ($R^2 = 0.93$) and Other—massive ($R^2 = 0.91$) (Fig. 4). While to a lesser extent, a positive relationship was also identified for *Acropora*—staghorn ($R^2 = 0.81$) and *Astreopora* ($R^2 = 0.82$) and weaker relationships were identified for *Goniastrea* ($R^2 = 0.77$) and *Porites*—massive ($R^2 = 0.75$) (Fig. 4, Table 1).

Models differed in their scaling relationships (Fig. 5), though there were similarities found between certain groups of morphotaxa. Tightly branching morphotaxa (*Acropora*—Other, *Pocillopora*, *Seriatopora* and *Stylophora*; see blue hues in Fig. 5) all follow very similar power relationships; however, this relationship is considerably different to the trajectory shared by encrusting corals (*Montipora* and Other-encrusting, see green hues in Fig. 5) and massive corals (see pink/purple hues in Fig. 5). These data provide insight into differences in the 3D surface area to colony maximum diameter ratios among morphotaxa.

An inherent consideration of this work is the uncertainty associated with model-derived estimates. To clearly present this to users we incorporated bands of probability into the key figures (HDIs 0.99, 0.95, 0.8, 0.5) (Figs. 3 & 4) to demonstrate the range over which the posterior distribution credibly lies. We also produced tables of predicted values (Emmeans) for each morphotaxon and the associated HDIs of each estimate (Supplementary material, Appendix 2, Tables S2-S16). Figures 3 & 4 show variability in HDI band width between morphotaxa, representing variation in model certainty. Trends of increasing HDI width at larger colony sizes were evident for most morphotaxa, especially for those with very large colony maximum diameters such as staghorn *Acropora*. Caution should therefore be taken when interpreting results for staghorn *Acropora* colonies at the larger end of the size continuum, or avoided if precise estimates are required. Variation in model certainty is likely related to

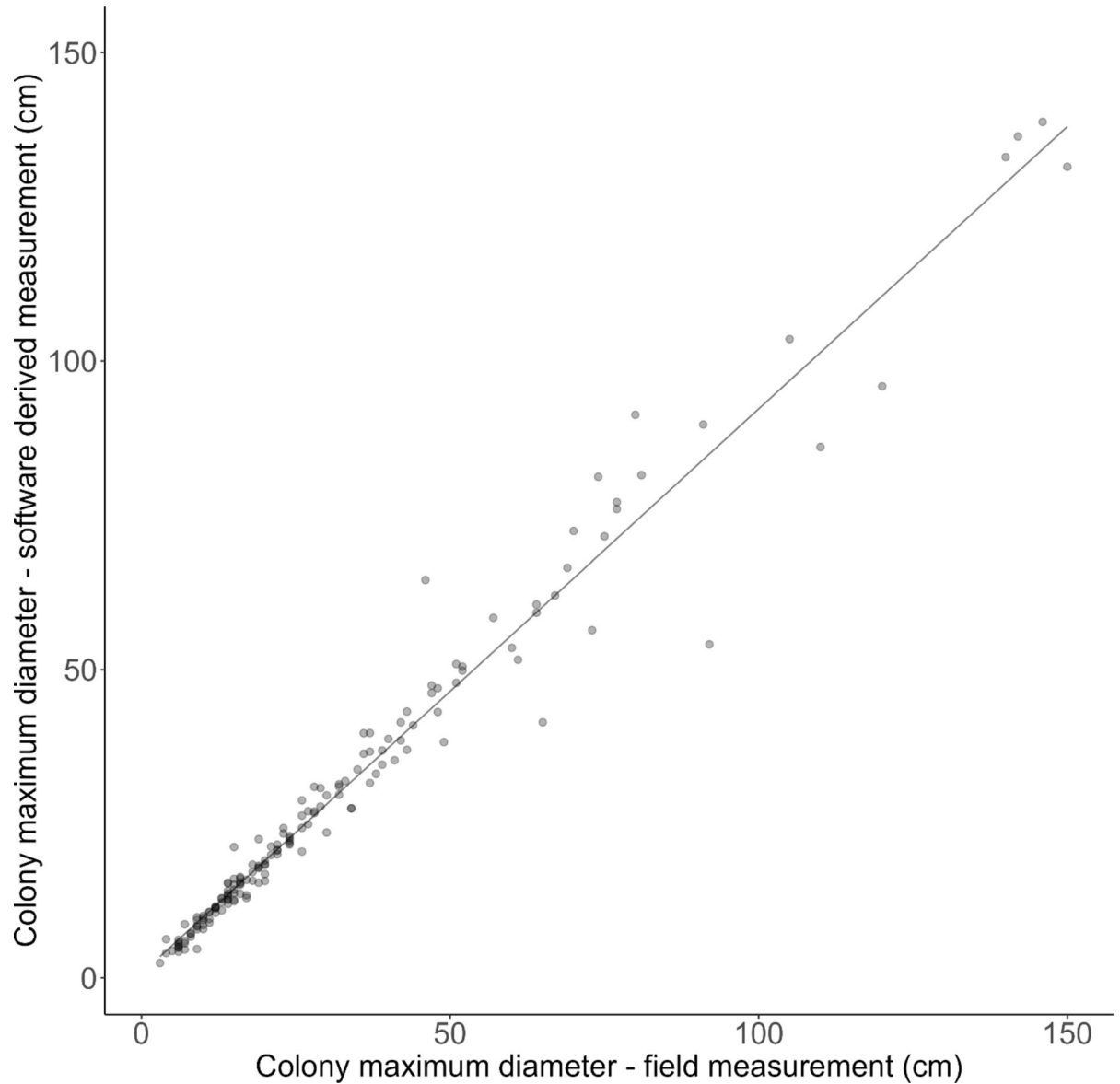


Fig. 2. Comparison of colony maximum diameter measurements taken from the field (x-axis) with colony maximum diameter derived from model reconstructions using Agisoft Metashape computer software (y-axis) ($R^2 = 0.97$, $n = 159$).

the extent of morphological plasticity within each morphotaxa which is why disproportionately higher numbers of replicates were sampled for morphotaxa containing complex and variable growth forms. Tables of predicted values (Emmeans) for each morphotaxon and the associated HDIs of estimates are presented in Supplementary material, Appendix 2, Tables S2-S16, which enable the interpretation of uncertainty levels associated with different colony sizes.

Discussion

Long-standing logistical constraints to accurately quantifying surface area of corals have hindered our understanding of their ecological function (e.g., McWilliam et al.⁴⁴). Here, we show that rapid field measurements of colony maximum diameter can be used to effectively predict total 3D surface area and projected 2D surface area for a diverse range of different corals, providing meaningful ecological metrics for various applications. By modelling detailed non-linear relationships between colony size and surface area for 15 different coral morphotaxa, we add to some previously established conversion metrics^{10,37,38} and create a valuable resource for reef monitoring programs. Previous studies have demonstrated the feasibility of converting measurements of colony maximum diameter to metrics of 3D and 2D surface area^{10,21,37,38}, however the scope of these published conversions have been restrictive, with the most wide-ranging study³⁷ producing relationships for seven morphotaxa groups which does not encompass all growth forms in the Indo-Pacific. The variation in scaling relationships that we have

Coral morphotaxon	Projected 2D surface area (PSA)		Total 3D surface area (TSA)	
	Model equation	R ²	Model equation	R ²
Acropora—other	$PSA = 0.448D^{2.046}$	0.99	$TSA = 0.837D^{2.459}$	0.95
Acropora—staghorn	$PSA = 0.186D^{1.981}$	0.84	$TSA = 0.838D^{2.024}$	0.81
Acropora—table	$PSA = 0.346D^{2.111}$	0.98	$TSA = 2.615D^{1.947}$	0.95
Astreopora	$PSA = 0.252D^{2.293}$	0.94	$TSA = 0.425D^{2.434}$	0.82
Fungia	$PSA = 0.790D^{1.910}$	0.99	$TSA = 0.587D^{2.440}$	0.96
Goniastrea	$PSA = 0.727D^{1.882}$	0.89	$TSA = 0.919D^{2.273}$	0.77
Lobophyllia	$PSA = 0.539D^{2.008}$	0.97	$TSA = 0.698D^{2.190}$	0.96
Montipora—encrusting	$PSA = 0.667D^{1.848}$	0.95	$TSA = 1.229D^{1.875}$	0.92
Pocillopora	$PSA = 0.324D^{2.133}$	0.94	$TSA = 0.709D^{2.50}$	0.95
Porites—massive	$PSA = 0.763D^{1.956}$	0.91	$TSA = 4.58D^{1.836}$	0.75
Seriatopora	$PSA = 0.359D^{2.093}$	0.97	$TSA = 0.831D^{2.451}$	0.97
Stylophora	$PSA = 0.420D^{2.46}$	0.96	$TSA = 0.878D^{2.413}$	0.96
Other—branching	$PSA = 0.107D^{2.346}$	0.94	$TSA = 0.651D^{2.212}$	0.96
Other—encrusting	$PSA = 0.639D^{1.876}$	0.96	$TSA = 0.802D^{2.024}$	0.93
Other—massive	$PSA = 0.611D^{2.00}$	0.96	$TSA = 0.573D^{2.414}$	0.91

Table 1. Model equations and Bayesian R² for predicting colony projected 2D surface area (PSA) and total 3D surface area (TSA) from field measurements of colony maximum diameter (D) for 15 coral morphotaxa. Additional information on model equation parameters (incl. 95% HDIs and SD for parameters $\alpha + \beta$) are presented in Supplementary material (Appendix 3, Table S17 & S18).

recorded between morphotaxa in this study (Fig. 5) demonstrates the importance of taxa-level data for obtaining the best possible model parameters.

The modelled power-relationships we established between colony maximum diameter and 3D surface area indicated very strong relationships (R² > 0.90) for 11 out of 15 of the morphotaxa. The four morphotaxa that exhibited lower model-fit values (R² = 0.75–0.89) were staghorn *Acropora*, *Astreopora*, *Goniastrea* and massive *Porites*, and the use of these four predictive models for obtaining surface area values should be approached with some caution. Surprisingly, *Astreopora*, *Goniastrea* and massive *Porites* have simple growth forms but were found to produce only moderately strong relationships, largely owing to irregular height to width ratios due to their susceptibility to partial mortality^{45,46}, obscuring the relationship between field measurement of planar diameter and surface area (see example images of massive *Porites* in Supplementary material, Appendix 4). For staghorn *Acropora*, confidence in posterior draws was found to be strong at smaller sizes but weakens considerably at larger colony sizes (> 80cm), likely due to the variability in branch density and hence surface area at larger colony sizes (see example images of staghorn *Acropora* in Supplementary material, Appendix 4). Thus, the use of these conversion metrics for very large colony sizes of staghorn *Acropora* should be avoided. For all other morphotaxa, surface area scaled well with size, and the conversion metrics can be used with relative confidence. In order for users to interpret model precision and confidence over the range of morphotaxa and colony sizes that they are working with, we have included tables presenting model uncertainty (Supplementary material, Appendix 2, tables S2–S16). An additional consideration of this study is that the morphological plasticity of conspecific corals that occur in accordance with environmental exposure (i.e., hydrodynamics, sedimentation^{47,48}) and depth^{49,50}, may affect the representativeness of the corals we imaged which were selected from just one location. As the corals selected represent the dominant growth forms within each morphotaxon (see Appendix 4, Supplementary Material), the presented relationships should sufficiently encompass corals from most other locations. However, practitioners working in different regions to this study should exercise caution when working with these conversion metrics. Additional model equations for morphotaxa not captured here and/or colonies from other tropical Indo-Pacific regions can be produced by replicating our methodology.

The relationships presented here have utility for a wide range of applications from small-scale studies of ecological processes to ecosystem modelling. At a colony level, applications could include the extrapolation of any processes which are standardized to biotic surface area such as symbiont density, chlorophyll concentration, and metabolic processes^{21,26,51,52}. Scaling up colony level processes to a reef scale via complementary field surveys or with remote sensing imagery would also be possible^{21,53}. Given that the surface area of corals is a known descriptor of tissue biomass, it can be a proxy for potential nutrient intake of coral predators⁵⁴. Refining our knowledge about the total tissue area availability (and total protein) for a given colony can provide insight into the underlying explanations for feeding preferences by key coral predators. For crown-of-thorns starfish (*Acanthaster* spp.), for which feeding preferences are well studied^{55–58}, there remains uncertainty around the basis of feeding choices where nutritional value and availability alone cannot explain preferences^{56,59}. This work has demonstrated the substantial variation of surface area to coral diameter ratios between taxa which may be a key factor underpinning the apparent feeding preferences. For example, our relationships show that a *Pocillopora* colony with a maximum diameter of 40cm is likely to have a total 3D surface area more than six times as large as the total 3D surface area of *Montipora* with the same colony maximum diameter (*Montipora*: 1150cm²; *Pocillopora*: 7,234cm²). Crown-of-thorns starfish feed by everting their stomach over coral structures and dissolving

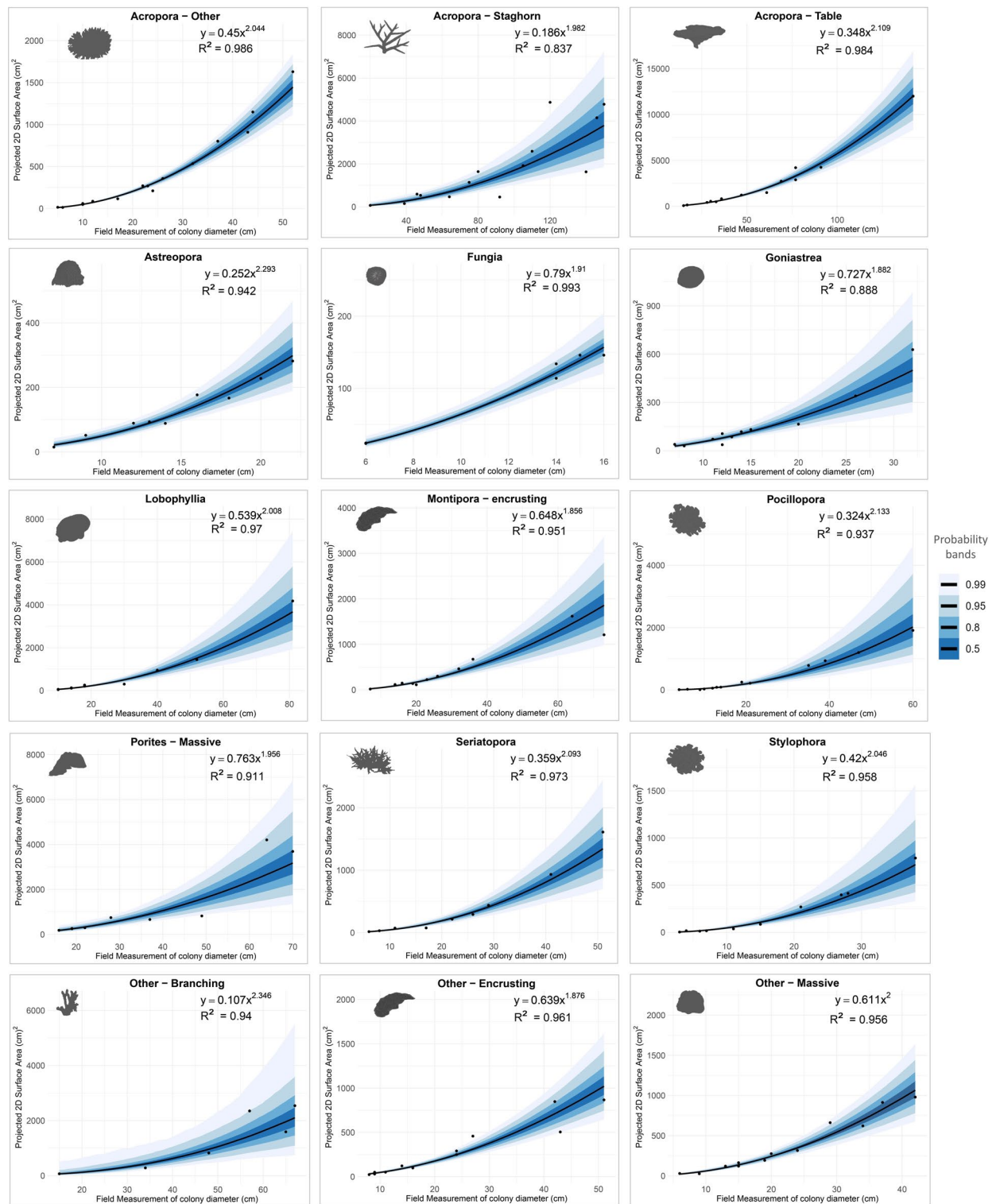


Fig. 3. Modelled power relationship between field measurements of colony maximum diameter (cm) and projected (2D) surface area (cm²) for 15 coral morphotaxa. Black lines represent median posterior distribution and bands represent 99%, 95%, 80% and 50% highest density intervals (HDIs) derived from posterior distribution. Model equations with parameters $\alpha + \beta$ are presented along with Bayesian R² value for each morphotaxon.

the entire tissue area⁵⁴, and so a high tissue area reward for limited effort of feeding and foraging may explain feeding choices, especially when feeding *efficiency* is thought to be the key determinant of preferences.

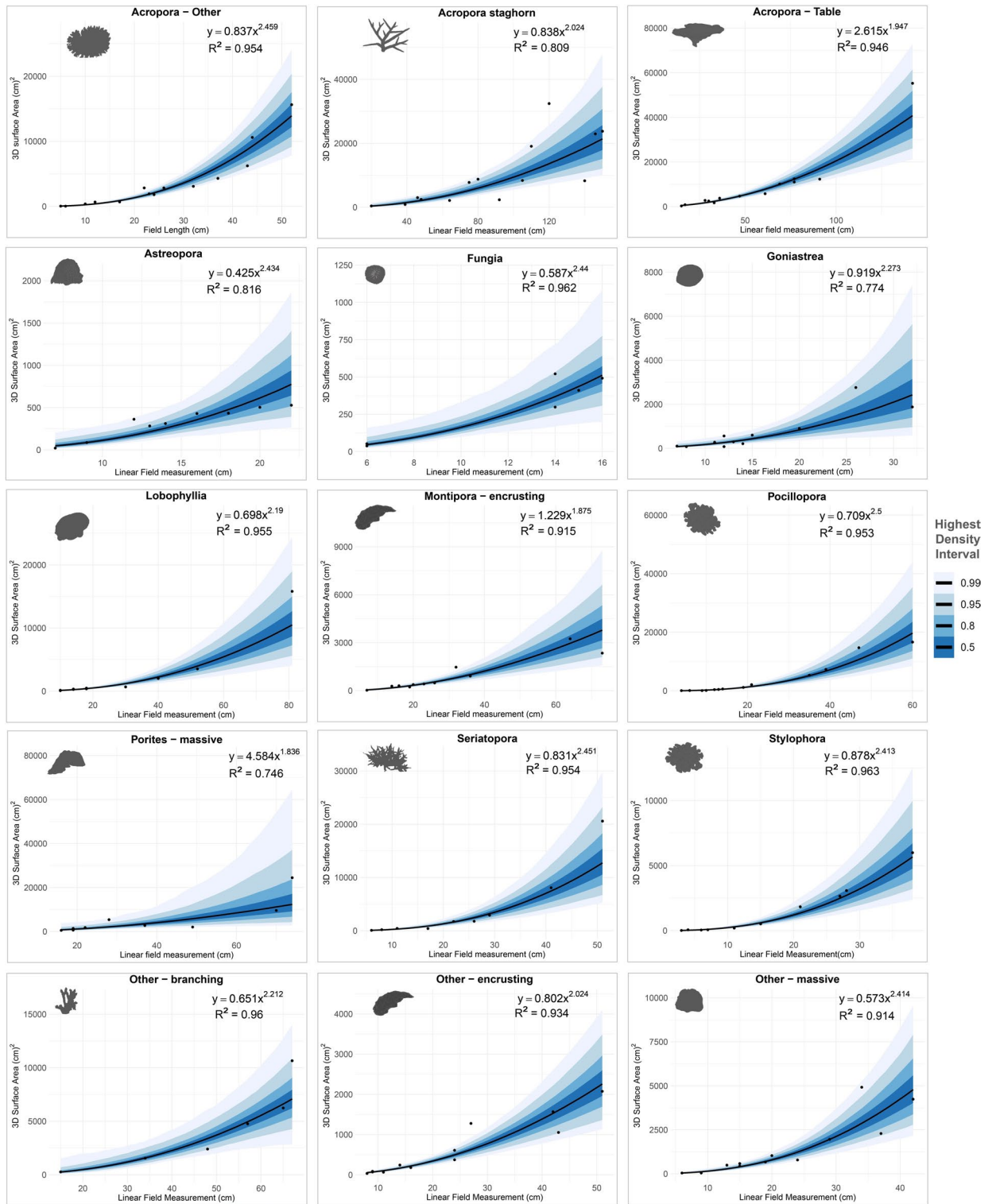


Fig. 4. Modelled power relationship between field measurements of colony maximum diameter (cm) and total (3D) surface area (cm²) for 15 coral morphotaxa. Black lines represent median posterior distribution and bands represent 99%, 95%, 80% and 50% highest density intervals (HDIs) derived from posterior distribution. Model equations with parameters $\alpha + \beta$ are presented along with Bayesian R² value for each morphotaxon.

Surface area metrics can also provide modelers and managers with valuable parameters related to reef growth, for example for modelling calcification rates of corals; a vital parameter in the calculation of carbonate budget models. With the increasing use of carbonate budgets as a method for evaluating reef status and trends in

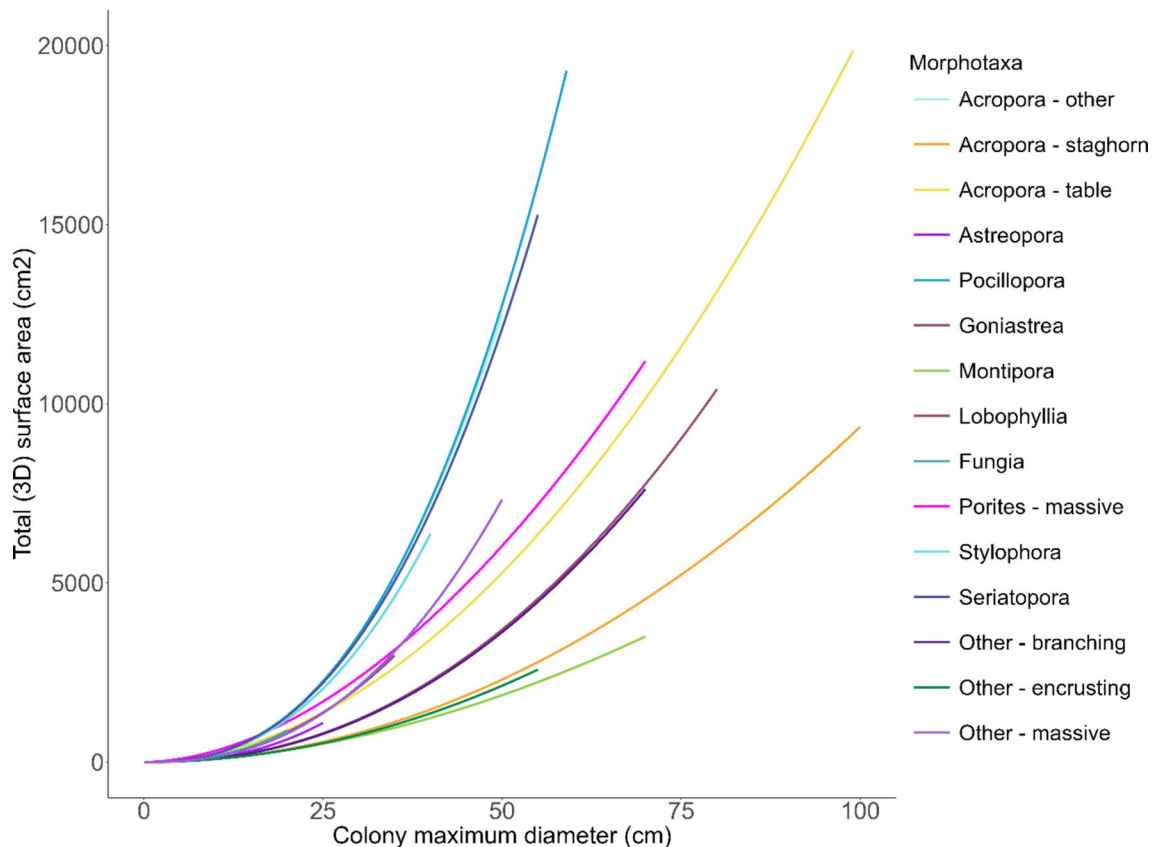


Fig. 5. Median lines of posterior distributions for modelled power relationships between colony maximum diameter and total (3D) surface area for 15 coral morphotaxa.

ecosystem function over time⁶⁰, methods that enable accurate and efficient surface area measurements of coral colonies, provide a useful contribution to reef-scale calcification modelling^{60–62}. An important development in the efficiency and scale of this work has been the development of Coral Colony Rugosity Indices (CCRI) by Husband et al.⁶¹ which enable calcification rates to be calculated from planar measurements of corals. These CCRI conversion metrics facilitate the conversion of datasets, including carbonate modelling of historic data. As a further development of this work, our study presents an alternative method for converting measurements of colony maximum diameter, derived from field data or images, to morphotaxon-specific surface area values. As such, a future application of this work could be combining the surface area values of corals (obtained using our conversion metrics) with species-specific calcification rates as an alternative approach for gaining high resolution estimates of coral carbonate production.

This work also has applications for studying temporal and spatial trends in coral growth rates. In coral growth studies, quantification of the 3D structure of individual colonies provides a more rigorous representation of total growth compared to linear colony measurements or planar projected areas⁶³. Studies of coral growth, in particular those that monitor outplanted corals from restoration activities, can often span large areas and include thousands of colonies^{64,65}. This paper presents an opportunity to conduct rapid field measurements of outplanted colonies and gain estimates of colony growth over time, especially as coral restoration and recovery research has gained major interest in recent years after impacts of cumulative disturbances^{66–68}.

Moreover this study has application for assessing additional aspects of coral demography, such as competition, fecundity, and partial mortality of corals. The surface area occupied by different coral species can be monitored to assess the dynamic interplay of coral growth and competition on a reef in 2D and 3D space, which is important for understanding coral community dynamics and their response to disturbance⁶⁹. In particular, monitoring space occupancy of corals after major disturbance events can further our understanding of recovery trajectories and inform ecological models. Surface area metrics can also provide insight into reproductive potential of corals, as coral morphology and size can be used as a proxy for reproductive potential of individuals⁷⁰. Using this approach to estimate surface area therefore provides a valuable tool for studying key processes that drive reef resilience and recovery.

Conclusion

Coral colony surface area is an important ecological parameter and serves as a fundamental determinant of physical and biological processes as well as ecosystem services. As such, there is a demand for obtaining highly resolved estimates of coral surface area. This method presents a process for rapidly gaining highly resolved morphotaxon-specific surface area estimates from easily obtained measurements of coral colony maximum

diameter. Large datasets of colony diameter measurements can be converted to surface area metrics using the model equations provided. Coral colony measurements can be collected in the field using tape measures or alternatively extracted from photographs (including historic image sets), enabling researchers to gather valuable surface area metrics without complex equipment or software. This approach cannot replicate the precision and accuracy of conducting photogrammetry on every colony, however, the benefit of scaling up to large datasets makes this trade-off worthwhile and this approach highly valuable. Key applications of this approach include the 1) extrapolation of processes standardized to biotic surface area (e.g., photosynthesis, calcification), 2) assessment of tissue biomass for ecological studies (e.g., coral predator ecology), 3) upscaling from colony-scale to reef carbonate production, 4) quantification of coral growth (e.g., for reef restoration monitoring), and 5) assessment of coral demographics and space competition.

Data availability

All data analysed as part of this study are available from Research JCU (<https://doi.org/10.25903/m2ap-4p06>), which will be released from embargo on publication. Contact data manager Josie Chandler josie.chandler@my.jcu.edu.au to request earlier access to this data.

Received: 29 May 2024; Accepted: 29 August 2024

Published online: 04 September 2024

References

- Luckhurst, B. E. & Luckhurst, K. Analysis of the influence of substrate variables on coral reef fish communities. *Mar Biol* **49**, 317–323 (1978).
- Graham, N. A. J. Habitat complexity: Coral structural loss leads to fisheries declines. *Current Biology* **24**, (2014).
- Almany, G. R. Differential effects of habitat complexity, predators and competitors on abundance of juvenile and adult coral reef fishes. *Oecologia* **141**, 105–113 (2004).
- Moberg, F. & Folke, C. Ecological goods and services of coral reef ecosystems. *Ecol. Econ.* **29**, (1999).
- Reguero, B. G. *et al.* The value of US coral reefs for flood risk reduction. *Nat Sustain* **4**, 688–698 (2021).
- Cruz-Trinidad, A., Aliño, P. M., Geronimo, R. C. & Cabral, R. B. Linking food security with coral reefs and fisheries in the coral triangle. *Coast. Manag.* **42**, 160–182 (2014).
- Eddy, T. D. *et al.* Global decline in capacity of coral reefs to provide ecosystem services. *One Earth* **4**, 1278–1285 (2021).
- Leujak, W. & Ormond, R. F. G. Comparative accuracy and efficiency of six coral community survey methods. *J. Exp. Mar. Biol. Ecol.* **351**, 168–187 (2007).
- Hill, J. & Wilkinson, C. *Methods for ecological monitoring of coral reefs.* (2004).
- House, J. E. *et al.* Moving to 3D: Relationships between coral planar area, surface area and volume. *PeerJ* **6**, (2018).
- Torres-Pulliza, D. *et al.* A geometric basis for surface habitat complexity and biodiversity. *Nat. Ecol. Evol.* **4**, 1495–1501 (2020).
- Fisher, W. S. Relating fish populations to coral colony size and complexity. *Ecol. Indic.* **148**, (2023).
- Komyakova, V., Munday, P. L. & Jones, G. P. Relative importance of coral cover, habitat complexity and diversity in determining the structure of reef fish communities. *PLoS One* **8**, (2013).
- Newman, S. P. *et al.* Reef flattening effects on total richness and species responses in the Caribbean. *J. Anim. Ecol.* **84**, 1678–1689 (2015).
- Ferrari, R. *et al.* 3D photogrammetry quantifies growth and external erosion of individual coral colonies and skeletons. *Sci. Rep.* **7**, (2017).
- Urbina-Barreto, I. *et al.* Quantifying the shelter capacity of coral reefs using photogrammetric 3D modeling: From colonies to reefscales. *Ecol. Indic.* **121**, (2021).
- Meiling, S., Muller, E. M., Smith, T. B. & Brandt, M. E. 3D photogrammetry reveals dynamics of stony coral tissue loss disease (SCTLD) lesion progression across a thermal stress event. *Front. Mar. Sci.* **7**, (2020).
- Lange, I. D., Molina-Hernández, A., Medellín-Maldonado, F., Perry, C. T. & Álvarez-Filip, L. Structure-from-motion photogrammetry demonstrates variability in coral growth within colonies and across habitats. *PLoS One* **17**, (2022).
- Odum, H. T. & Odum, E. P. *Trophic structure and productivity of a windward coral reef community on Eniwetok atoll.* vol. 25 (1955).
- Dahl, A. L. Surface area in ecological analysis: Quantification of benthic coral-reef algae. *Mar. Biol.* **23**, 239–249 (1973).
- Holmes, G. Estimating three-dimensional surface areas on coral reefs. *J. Exp. Mar. Biol. Ecol.* **365**, 67–73 (2008).
- Alcala, M. L. R. & Vogt, H. Approximation of coral reef surfaces using standardized growth forms and video counts. in *Proc. 8th Int. Coral Reef. Symp.* vol. 2 (1997).
- Laforsch, C. *et al.* A precise and non-destructive method to calculate the surface area in living scleractinian corals using X-ray computed tomography and 3D modeling. *Coral Reefs* **27**, 811–820 (2008).
- Marsh, J. A. *Primary productivity of reef-building calcareous red algae.* *Source: Ecol.* vol. 51 (1970).
- Stimson, J. & Kinzie, R. A. The temporal pattern and rate of release of zooxanthellae from the reef coral *Pocillopora damicornis* (Linnaeus) under nitrogen-enrichment and control conditions. *Mar. Biol. Ecol.* **153**, 63 (1991).
- Hoegh-Guldberg, O. A method for determining the surface area of corals. *Coral Reefs* **7**, 113–116 (1988).
- Meyer, J. L. & Schultz, E. T. Tissue condition and growth rate of corals associated with schooling fish. *Limnol. Oceanogr.* **30**, 157–166 (1985).
- Naumann, M. S., Niggel, W., Laforsch, C., Glaser, C. & Wild, C. Coral surface area quantification-evaluation of established techniques by comparison with computer tomography. *Coral Reefs* **28**, 109–117 (2009).
- Drap, P. Underwater photogrammetry for archaeology. in *Special Applications of Photogrammetry* (InTech, 2012). <https://doi.org/10.5772/33999>.
- Figueira, W. *et al.* Accuracy and precision of habitat structural complexity metrics derived from underwater photogrammetry. *Remote Sens. (Basel)* **7**, 16883–16900 (2015).
- Urbina-Barreto, I. *et al.* Which method for which purpose? A comparison of line intercept transect and underwater photogrammetry methods for coral reef surveys. *Front. Mar. Sci.* **8**, (2021).
- Lechene, M. A. A. *et al.* Evaluating error sources to improve precision in the co-registration of underwater 3D models. *Ecol. Inform.* **81**, (2024).
- Ferrari, R. *et al.* Advances in 3D habitat mapping of marine ecosystem ecology and conservation. *Front. Mar. Sci.* **8**, (2022).
- Bythell, J., Pan, P. & Lee, J. Three-dimensional morphometric measurements of reef corals using underwater photogrammetry techniques. *Coral Reefs* **20**, 193–199 (2001).
- Remmers, T. *et al.* Close-range underwater photogrammetry for coral reef ecology: A systematic literature review. *Coral Reefs* **43**, 35–52 (2024).

36. Rossi, P., Castagnetti, C., Capra, A., Brooks, A. J. & Mancini, F. Detecting change in coral reef 3D structure using underwater photogrammetry: critical issues and performance metrics. *Appl. Geomat.* **12**, 3–17 (2020).
37. Aston, E. A., Duce, S., Hoey, A. S. & Ferrari, R. A Protocol for extracting structural metrics from 3D reconstructions of corals. *Front. Mar. Sci.* **9**, (2022).
38. Courtney, L. A., Fisher, W. S., Raimondo, S., Oliver, L. M. & Davis, W. P. Estimating 3-dimensional colony surface area of field corals. *J. Exp. Mar. Biol. Ecol.* **351**, 234–242 (2007).
39. Dornelas, M., Madin, J. S., Baird, A. H. & Connolly, S. R. Allometric growth in reef-building corals. *Proc. R. Soc. B Biol. Sci.* **284**, (2017).
40. Hartig, F. DHARMA: residual diagnostics for hierarchical (multi-level/mixed) regression models. (2018).
41. Lenth, R., Singmann, H., Buerkner, P. & Herve, M. Emmeans: Estimated marginal means, aka least-squares means. (2018).
42. R Core Team. R: A language and environment for statistical computing. *R Foundation for Statistical Computing* (2021).
43. Bürkner, P. C. brms: An R package for Bayesian multilevel models using Stan. *J. Stat. Softw.* **80**, (2017).
44. McWilliam, M., Pratchett, M. S., Hoogenboom, M. O. & Hughes, T. P. Deficits in functional trait diversity following recovery on coral reefs. *Proc. R. Soc. B Biol. Sci.* **287**, (2020).
45. Jones, N., Pratchett, M., Milligan, R. & Gilliam, D. High incidence of partial colony mortality constrains realized growth for three coral species in southeast Florida. *Mar. Ecol. Prog. Ser.* **721**, 59–70 (2023).
46. Burn, D., Matthews, S., Pisapia, C., Hoey, A. S. & Pratchett, M. S. Changes in the incidence of coral injuries during mass bleaching across Australia's Coral Sea Marine Park. *Mar. Ecol. Prog. Ser.* **682**, 97–109 (2022).
47. Doszpot, N. E., McWilliam, M. J., Pratchett, M. S., Hoey, A. S. & Figueira, W. F. Plasticity in three-dimensional geometry of branching corals along a cross-shelf gradient. *Diversity (Basel)* **11**, (2019).
48. Million, W. C. *et al.* Evidence for adaptive morphological plasticity in the Caribbean coral, *Acropora cervicornis*. *Proc. Natl. Acad. Sci. USA* **119**, (2022).
49. Hoogenboom, M. O., Connolly, S. R. & Anthony, K. R. N. Interactions between morphological and physiological plasticity optimize energy acquisition in corals. *Ecology* **89**, 1144–1154 (2008).
50. Anthony, K. R. N., Hoogenboom, M. O. & Connolly, S. R. Adaptive variation in coral geometry and the optimization of internal colony light climates. *Funct. Ecol.* **19**, 17–26 (2005).
51. Veal, C. J., Holmes, G., Nunez, M., Hoegh-Guldberg, O. & Osborn, J. A comparative study of methods for surface area and three dimensional shape measurement of coral skeletons. *Limnol. Oceanogr. Methods* **8**, 241–253 (2010).
52. Fisher, W. S. *et al.* Characterizing coral condition using estimates of three-dimensional colony surface area. *Environ. Monit. Assess* **125**, 347–360 (2007).
53. Andréfouët, S. & Payri, C. Scaling-up carbon and carbonate metabolism of coral reefs using in-situ data and remote sensing. *Coral Reefs* **19**, 259–269 (2001).
54. Keesing, J. K. Feeding biology of the crown-of-thorns starfish, *Acanthaster planci* (Linnaeus). (Townsville, 1990).
55. De'ath, G. & Moran, P. J. Factors affecting the behaviour of crown-of-thorns starfish (*Acanthaster planci* L.) on the Great Barrier Reef: 2. Feeding preferences. *J. Exp. Mar. Biol. Ecol.* **220**, (1998).
56. Keesing, J. K. Optimal foraging theory explains feeding preferences in the western pacific crown-of-thorns sea star *Acanthaster* sp. *Biol. Bull.* **241**, 303–329 (2021).
57. Keesing, J. K. & Lucas, J. S. Field measurement of feeding and movement rates of the crown-of-thorns starfish *Acanthaster planci* (L.). *Mar. Biol. Ecol.* **156**, 89–104 (1992).
58. Ormond, R. F. G., Hanscomb, N. J. & Beach, D. H. Food selection and learning in the crown-of-thorns starfish, *Acanthaster planci* (L.). *Mar Behav Physiol* **4**, (1976).
59. Johansson, C. L., Francis, D. S. & Uthicke, S. Food preferences of juvenile corallivorous crown-of-thorns (*Acanthaster planci*) sea stars. *Mar. Biol.* **163**, 1–7 (2016).
60. Lange, I. D., Perry, C. T. & Alvarez-Filipe, L. Carbonate budgets as indicators of functional reef “health”: A critical review of data underpinning census-based methods and current knowledge gaps. *Ecol. Indic.* **110**, (2020).
61. Husband, E., Perry, C. T. & Lange, I. D. Estimating rates of coral carbonate production from aerial and archive imagery by applying colony scale conversion metrics. *Coral Reefs* **41**, 1199–1209 (2022).
62. Perry, C. T. *et al.* Estimating rates of biologically driven coral reef framework production and erosion: A new census-based carbonate budget methodology and applications to the reefs of Bonaire. *Coral Reefs* **31**, 853–868 (2012).
63. Holmes, G., Ortiz, J., Kaniewska, P. & Johnstone, R. Using three-dimensional surface area to compare the growth of two Pocilloporid coral species. *Mar. Biol.* **155**, 421–427 (2008).
64. Foo, S. A. & Asner, G. P. Scaling up coral reef restoration using remote sensing technology. *Front. Mar. Sci.* **6**, (2019).
65. Maya, P. H. M., Smit, K. P., Burt, A. J. & Frias-Torres, S. Large-scale coral reef restoration could assist natural recovery in Seychelles Indian Ocean. *Nat. Conserv.* **16**, 1–17 (2016).
66. Bozec, Y. M. *et al.* Cumulative impacts across Australia's Great barrier reef: A mechanistic evaluation. *Ecol. Monogr.* **92**, (2022).
67. Mudge, L. & Bruno, J. F. Disturbance intensification is altering the trait composition of Caribbean reefs, locking them into a low functioning state. *Sci. Rep.* **13**, (2023).
68. Pratchett, M. S., Heron, S. F., Mellin, C. & Cumming, G. S. Recurrent mass-bleaching and the potential for ecosystem collapse on Australia's great barrier reef. in *Ecosystem Collapse and Climate Change* (eds. Canadell, J. G. & Jackson, R. B.) 265–289 (Springer, 2021). https://doi.org/10.1007/978-3-030-71330-0_10.
69. Cresswell, A. K., Thomson, D. P., Haywood, M. D. E. & Renton, M. Frequent hydrodynamic disturbances decrease the morphological diversity and structural complexity of 3D simulated coral communities. *Coral Reefs* **39**, 1147–1161 (2020).
70. Álvarez-Noriega, M. *et al.* Fecundity and the demographic strategies of coral morphologies. *Ecology* **97**, 3485–3493 (2016).

Acknowledgements

Funding was provided by the COTS Control Innovation Program and the ARC Centre of Excellence for Coral Reef Studies. Thanks to Anne Hoggett, Lyle Vail and other Lizard Island Research Station staff for significant logistical support. We acknowledge the Dingaal Aboriginal people, the Traditional Owners of Lizard Island (Jiigurru), and their continuing connection to their land and sea country.

Author contributions

M.S.P. designed the overarching study and J.F.C., M.S.P., W.F.F., P.C.D. and D.B. conceptualised the manuscript. A.J., D.B., J.F.C. and W.F.F. collected the data. J.F.C. and A.P. performed the analyses. J.F.C. wrote the manuscript, with contributions by P.C.D., M.S.P., W.F.F., A.J., A.P., and D.B. All authors reviewed the manuscript.

Competing interests

The authors declare no competing interests.

Additional information

Supplementary Information The online version contains supplementary material available at <https://doi.org/10.1038/s41598-024-71580-3>.

Correspondence and requests for materials should be addressed to J.F.C.

Reprints and permissions information is available at www.nature.com/reprints.

Publisher's note Springer Nature remains neutral with regard to jurisdictional claims in published maps and institutional affiliations.

Open Access This article is licensed under a Creative Commons Attribution-NonCommercial-NoDerivatives 4.0 International License, which permits any non-commercial use, sharing, distribution and reproduction in any medium or format, as long as you give appropriate credit to the original author(s) and the source, provide a link to the Creative Commons licence, and indicate if you modified the licensed material. You do not have permission under this licence to share adapted material derived from this article or parts of it. The images or other third party material in this article are included in the article's Creative Commons licence, unless indicated otherwise in a credit line to the material. If material is not included in the article's Creative Commons licence and your intended use is not permitted by statutory regulation or exceeds the permitted use, you will need to obtain permission directly from the copyright holder. To view a copy of this licence, visit <http://creativecommons.org/licenses/by-nc-nd/4.0/>.

© The Author(s) 2024